

Evidence for the Role of DNA Strand Passage in the Mechanism of Action of Microcin B17 on DNA Gyrase[†]

Olivier A. Pierrat and Anthony Maxwell*

Department of Biological Chemistry, John Innes Centre, Norwich Research Park, Colney, Norwich NR4 7UH, United Kingdom

Received October 1, 2004; Revised Manuscript Received December 17, 2004

ABSTRACT: Microcin B17 (MccB17) is a DNA gyrase poison; in previous work, this bacterial toxin was found to slowly and incompletely inhibit the reactions of supercoiling and relaxation of DNA by gyrase and to stabilize the cleavage complex, depending on the presence of ATP and the DNA topology. We now show that the action of MccB17 on the gyrase ATPase reaction and cleavage complex formation requires a linear DNA fragment of more than 150 base pairs. MccB17 is unable to stimulate the ATPase reaction by stabilizing the weak interactions between short linear DNA fragments (70 base pairs or less) and gyrase, in contrast with the quinolone ciprofloxacin. However, MccB17 can affect the ATP-dependent relaxation of DNA by gyrase lacking its DNA-wrapping or ATPase domains. From these findings, we propose a mode of action of MccB17 requiring a DNA molecule long enough to allow the transport of a segment through the DNA gate of the enzyme. Furthermore, we suggest that MccB17 may trap a transient intermediate state of the gyrase reaction present only during DNA strand passage and enzyme turnover. The proteolytic signature of MccB17 from trypsin treatment of the full enzyme requires DNA and ATP and shows a protection of the C-terminal 47-kDa domain of gyrase, indicating the involvement of this domain in the toxin mode of action and consistent with its proposed role in the mechanism of DNA strand passage. We suggest that the binding site of MccB17 is in the C-terminal domain of GyrB.

Microcin B17 (MccB17)¹ is a 3.1-kDa peptide antibiotic produced by *Escherichia coli* (1, 2) that displays a high level of posttranslational modification, with the formation of thiazole and oxazole heterocycles (Figure 1C) (2–7). Evidence that DNA gyrase is the intracellular target of MccB17 came from the observation that MccB17 traps the gyrase–DNA complex in its cleavage complex form, leading to the accumulation of double-stranded DNA breaks, inhibition of DNA replication, and cell death (8–10). Furthermore, in addition to uptake-deficient mutants, a mutation of the DNA gyrase B subunit (Trp⁷⁵¹ → Arg) was identified as resistant to MccB17, confirming that gyrase is the cellular target of the toxin (8). In vitro experiments showed that the gyrase–MccB17 complex on DNA blocks the passage of DNA polymerase (10). In addition, it has been found that, under specific conditions, MccB17 can inhibit the ATP-dependent supercoiling and ATP-independent relaxation of DNA by gyrase (11, 12).

DNA gyrase is a DNA topoisomerase that negatively supercoils DNA using ATP hydrolysis as a source of energy. The active enzyme is an A₂B₂ heterotetramer with the A subunit largely responsible for DNA wrapping and DNA breakage–reunion and the B subunit responsible for ATP hydrolysis and the interaction with GyrA and DNA. To

supercoil DNA, gyrase wraps a double-stranded segment of DNA around itself, cleaves both strands, transports the wrapped DNA through the break, and reseals the DNA (for recent reviews see refs 13 and 14). The cleaved DNA segment is known as the “gate” or “G” segment, and the segment that is passed through the enzyme is known as the “transported” or “T” segment (15). High-resolution structures of certain domains of gyrase are now available. GyrA consists of an N-terminal domain comprising the active site tyrosine and residues involved in interaction with quinolones and a C-terminal domain involved in DNA wrapping. High-resolution crystal structures of both of these domains are available (16, 17). GyrB comprises an N-terminal ATPase domain and a C-terminal domain involved in interactions with GyrA and DNA; a high-resolution crystal structure of the ATPase domain is available (18). A complex including just the N-terminus of GyrA (GyrA59) and GyrB can carry out ATP-dependent DNA relaxation, low levels of ATP-independent DNA relaxation, but not DNA supercoiling (19). A complex including just the C-terminus of GyrB (GyrB47) and GyrA can perform ATP-independent DNA relaxation but not DNA supercoiling (20, 21). Because gyrase is an essential enzyme in bacteria and is not present in humans, this enzyme is extensively studied as a target for antibacterial agents, such as the aminocoumarins and quinolones, and the bacterial toxins CcdB and MccB17 (22). Despite the significant amount of knowledge accumulated on MccB17, its mode of action on gyrase is still not known.

In previous work (12), we found that MccB17 could not block the gyrase reaction immediately, as inhibition of the DNA supercoiling and DNA relaxation reactions by gyrase

[†] This work was supported by a grant from the Biotechnology and Biological Sciences Research Council (to A.M.).

* To whom correspondence should be addressed. Tel: +44 1603 450771. Fax: +44 1603 450018. E-mail: tony.maxwell@bbsrc.ac.uk.

¹ Abbreviations: bp, base pairs; CFX, ciprofloxacin; GyrA and GyrB, DNA gyrase A and B subunits; MccB17, microcin B17; Novo, novobiocin; topo, DNA topoisomerase.

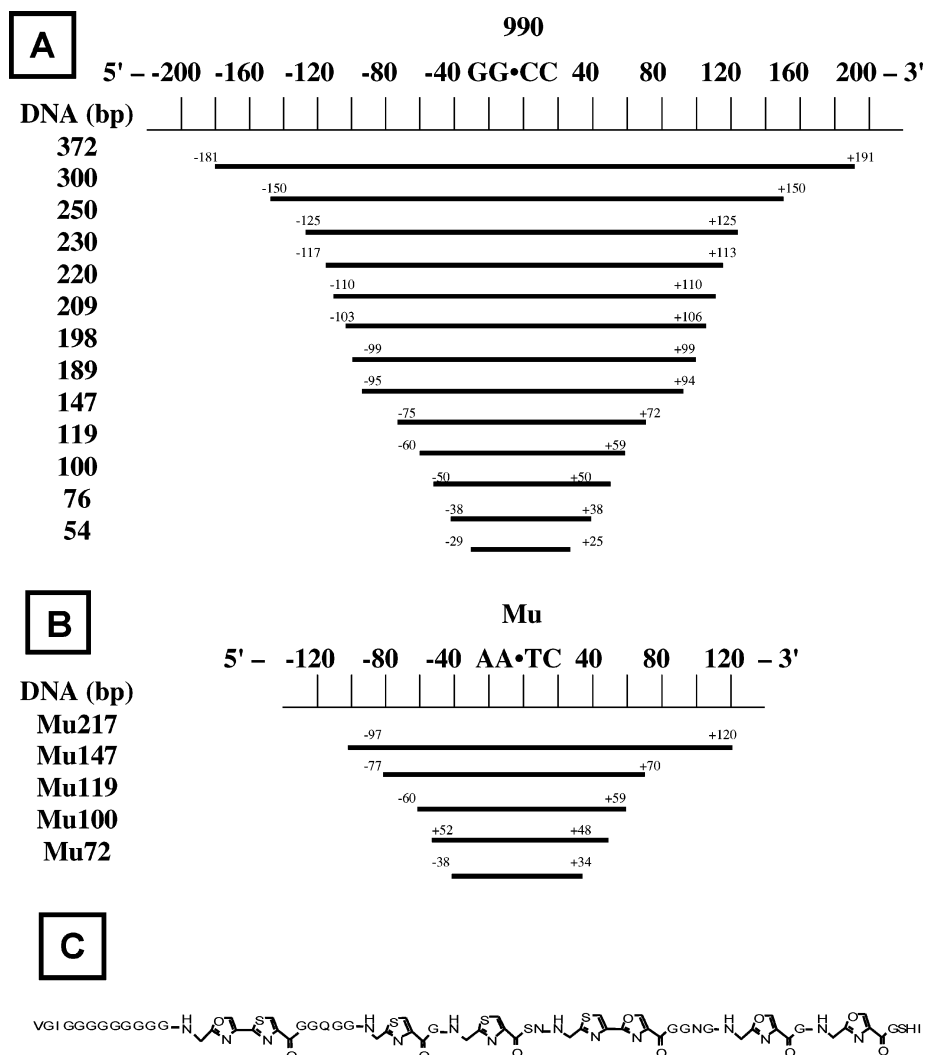


FIGURE 1: DNA fragments used in this study. Black dots indicate the center of the major quinolone-induced cleavage site in (A) plasmid pBR322 [990 site (27)] and (B) pMP1625 [Mu site (28, 36)]. The figure shows the fragment sizes with the distances in base pairs from (A) the pBR322 cleavage site at position 990 and (B) the bacteriophage Mu cleavage site at position 17875 (54). (C) Structure of MccB17.

only occurs when the enzyme has completed several catalytic cycles, and MccB17 only decreased the rate of DNA strand passage by a factor of ~ 3 . Moreover, MccB17 increased the rate of cleavage of the second strand of DNA, and this cleavage-complex stabilization by MccB17 was greatly dependent on the presence of ATP and the topological state of the DNA substrate. The findings of these experiments prompted us to explore the possibility that the mode of action of MccB17 on gyrase involves DNA strand passage through the enzyme. To shed more light on the interaction of MccB17 with gyrase, the present work investigates the characteristics of ATP hydrolysis by the enzyme-toxin complex. After showing that the inhibitory effect of MccB17 on ATP hydrolysis by gyrase is dependent on the presence of DNA, we use the ATPase reaction of gyrase to probe the relationship between DNA length and the extent of inhibition by MccB17. To complement the findings of the ATPase reaction, we also investigate the DNA length requirement of the MccB17-induced cleavage reaction, as well as the toxin effects on DNA relaxation by the A59₂B₂ enzyme, lacking the DNA wrapping domain, and the A₂B₄₇ enzyme, lacking the ATPase domain. Our results indicate that MccB17 action depends on the presence of a linear DNA fragment long enough to permit a segment of DNA to be

passed through the enzyme, while the wrapping and ATPase domains of gyrase are not essential for toxin action. Finally, using limited proteolysis experiments, we found that binding of MccB17 to the full (A₂B₂) enzyme-DNA complex induces a protection of the C-terminal 47-kDa domain of GyrB.

MATERIALS AND METHODS

Materials. GyrA and GyrB were purified as previously described (23). GyrB was a gift of Mr. Sylvain Mitelheiser (John Innes Centre); GyrA and relaxed and supercoiled pBR322 DNA were gifts of Mrs. Alison Howells (John Innes Enterprises). Mouse monoclonal antibody directed against the C-terminal domain of GyrB (GyrB47) was used at 1/1000 dilution in Western blots, according to the manufacturer's instructions (John Innes Enterprises). The 59-kDa N-terminal GyrA fragment and the 47-kDa C-terminal GyrB fragment (gift from Dr. Clare Smith) were prepared as described previously (24, 25). DNA topoisomerase IV was a gift of Dr. Ruth Flatman (John Innes Centre). Ciprofloxacin, novobiocin, and trypsin (Sigma) were dissolved in water. Microcin B17 was purified and dissolved in Me₂SO as described previously (26). Linear pBR322 was prepared by digestion of the supercoiled form with *Eco*RI, followed by ethanol

precipitation and resuspension in 10 mM Tris-HCl (pH 7.5) and 1 mM EDTA. Linear DNA fragments, listed in Figure 1, were obtained by PCR using Ampli Taq Gold DNA polymerase (Applied Biosystems), ~20 bp oligoprimers (Sigma-Genosys), and two different templates: pBR322, containing the preferred quinolone-induced gyrase cleavage site at 990 bp [Figure 1A (27)], and pMP1625, a pBR322-based plasmid containing a 1.4 kb *Bam*HI–*Cla*I fragment comprising the strong gyrase site from the center of the bacteriophage Mu genome at the *Bam*HI site of pBR322 [Figure 1B (28)]. Each PCR product was checked on a 1% agarose gel for a single DNA band of the expected size and purified using the Qiaquick PCR purification kit (≥ 100 bp) or Qiaquick nucleotide removal kit (<100 bp) from Qiagen. DNA concentrations were quantified by UV absorption at 260 nm. The amount of template used in PCR reactions (1 ng/ μ L) accounted for ~1% of the concentration of the purified DNA product (60–120 ng/ μ L), was not visible on the gel, and did not interfere in the enzyme assays.

Enzyme Assays. ATP hydrolysis by DNA gyrase was linked to the oxidation of NADH using a pyruvate kinase (PK)/lactate dehydrogenase (LDH) coupled-enzyme assay and measured at 340 nm on a Spectramax Plus microplate reader (Molecular Devices). The ATPase assay was similar to that described previously (29), with some modifications. Each 100 μ L reaction contained 50 mM Tris-HCl (pH 7.5), 24 mM KCl, 5 mM MgCl₂, 6.5% (w/v) glycerol, 4 mM dithiothreitol, 0.4 mM NADH, 0.8 mM phosphoenolpyruvate, 1% (v/v) PK/LDH mix (Sigma), 40–80 nM gyrase enzyme, and 5% Me₂SO, with or without MccB17 or CFX generally at 30 μ M, unless stated. Where indicated, the reaction included novobiocin at 0.05 or 1 μ M. The reactions were measured in the presence or the absence of linear DNA of lengths varying from 54 to 4362 bp (full-length pBR322) and either at a fixed concentration of 10 μ g/mL or at a varied concentration between 0.5 and 30 μ g/mL. Reactions were initiated by the addition of 2 mM Mg•ATP and measured at 25 °C over 1.5 h. Errors bars were omitted in Figures 4–7 for better clarity; each ATPase assay was repeated at least twice, and standard deviations of data points were less than or equal to 10%.

Cleavage of small linear DNA fragments by gyrase was assayed under conditions similar to those reported earlier for the closed-circular plasmid (10, 12, 30), except that the reactions contained 200 nM gyrase, ~10 μ g/mL linear DNA (60–200 nM, depending on the size), 5 mM MgCl₂, 2 mM Mg•ATP, and 4% Me₂SO, with or without 30 μ M MccB17 or CFX. After incubation at 25 °C for 2 h, the reactions were treated with SDS and proteinase K as described previously (10, 30). DNA products were analyzed by electrophoresis through 8% polyacrylamide gels, and the intensity of the DNA bands was quantified as described previously (12).

ATP-dependent relaxation of negatively supercoiled DNA by the A592B₂ enzyme (gyrase lacking the DNA-wrapping domain) was as previously described (19), except that each 30 μ L reaction contained 20 mM KCl, 1.7 mM ATP, 20 μ g/mL (7.1 nM) negatively supercoiled pBR322, and 2.5% Me₂SO, with or without 30 μ M MccB17. Reactions were started by the addition of 20 nM enzyme and incubated at 25 °C for 4 h. For ATP-independent DNA relaxation, ATP was omitted, and the enzyme concentration was 80 nM. DNA cleavage was measured by treating reactions with SDS and

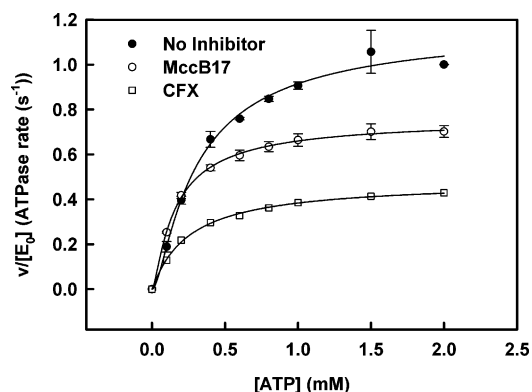


FIGURE 2: Effects of a saturating concentration of MccB17 or CFX on the kinetics of ATP hydrolysis by gyrase. Each reaction contains 44 nM GyrB dimer, 80 nM GyrA dimer, 7.5 nM linear pBR322, and 5% Me₂SO, with or without 30 μ M MccB17 or 100 μ M CFX. Reactions were initiated by adding ATP (0.1–2 mM), and the rate of ATP hydrolysis was measured at 25 °C in a PK/LDH coupled-enzyme assay (29). Data are fitted to eq 1 described in the Results section.

proteinase K and analyzing the reaction products on agarose gels, as previously described (10, 30). Cleavage assays and ATP-independent relaxation of negatively supercoiled DNA by A₂B₄₇₂ (47 nM) enzyme (gyrase lacking the ATPase domain) were performed at 25 °C for 3–6 h under the same conditions as previously described for the full gyrase enzyme (12).

Limited Proteolysis. Proteolysis experiments were performed as described previously (31), with some modifications. Reactions contained 0.3 mg/mL gyrase (A₂B₂ enzyme) and 0.24 mg/mL linear pBR322 DNA in 50 mM Tris-HCl (pH 7.5), 24 mM KCl, 5 mM MgCl₂, 4 mM dithiothreitol, 6.5% (w/v) glycerol, 3.3% Me₂SO, and 2.5 mM Mg•ATP. When present, MccB17 was included at 40 μ M. After incubation for 1 h at 25 °C, trypsin was added at a final concentration of 100–500 μ g/mL and the proteolysis allowed to proceed for 1 h at 37 °C. Samples were quenched by adding an equal volume of 125 mM Tris-HCl (pH 6.8), 20% (w/v) glycerol, 4% (w/v) SDS, 10% (v/v) β -mercaptoethanol, and 0.004% (w/v) bromophenol blue and boiling for 5 min. The products were analyzed by SDS–PAGE.

RESULTS

Kinetics of ATP Hydrolysis in the Presence of MccB17.

Previous work from our laboratory suggested that there was no significant effect of MccB17 on both DNA-dependent and DNA-independent ATPase activities of gyrase (10). In the present work, we confirmed that MccB17 (up to 50 μ M) does not affect the ATPase activity of GyrB or gyrase (A₂B₂) in the absence of DNA (data not shown). However, we were able to detect inhibition of the gyrase ATPase reaction in the presence of DNA. Results presented in Figure 2 show that, at saturating concentrations (30 μ M), MccB17 could inhibit the rate of ATP hydrolysis at ATP concentrations above 0.2 mM, with a maximal inhibition at 1.5–2 mM ATP. Fitting of the data in Figure 2 to the Michaelis–Menten equation shows that MccB17 lowered the apparent K_M and V_{max} for ATP by 2.3-fold and 1.6-fold, respectively. In comparison, saturating concentrations of CFX (100 μ M) decreased the apparent K_M and V_{max} by 1.6-fold and 2.7-fold, respectively. Although the Michaelis–Menten equation

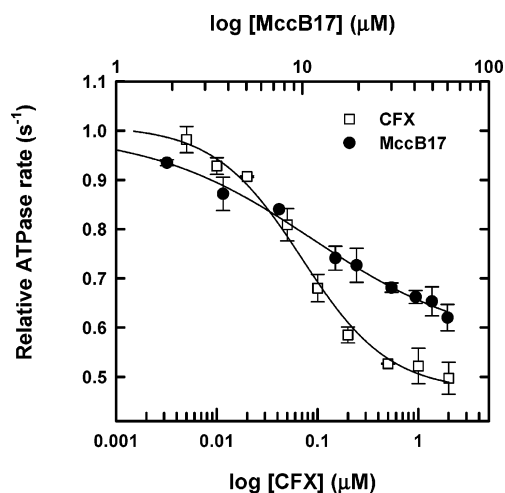
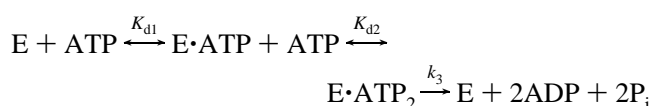


FIGURE 3: Effects of increasing concentrations of MccB17 or CFX on the gyrase ATPase reaction. Reactions were measured at 25 °C and contained 48 nM gyrase, 7.5 nM pBR322, 2 mM ATP, and 5% Me₂SO. ATPase activity is expressed relative to the rate in the absence of inhibitor (equal to 1 s⁻¹), and curves are from the fit to eq 2.

can be used to analyze the ATP hydrolysis reaction of gyrase (32, 33), this is a simplification as it is known that two binding sites for ATP are present per enzyme heterodimer, and nucleotide binding and hydrolysis at the two sites are not independent (29, 33). We therefore fitted the data in Figure 2 to the equation reported previously (34) that accounts for the two ATP-binding sites of gyrase:

$$\frac{\nu}{[E_0]} = \frac{2k_3[ATP]^2}{[ATP]^2 + K_{d2}[ATP] + K_{d1}K_{d2}} \quad (1)$$

where ν is the rate of ATP hydrolysis, $[E_0]$ is the total concentration of enzyme in the reaction, and K_{d1} , K_{d2} , and k_3 are equilibrium dissociation constants and a first-order rate constant, according to the reaction scheme:



Although the experimental data (Figure 2) were better fitted by eq 1 than by the Michaelis–Menten equation, large standard errors were obtained on the equilibrium dissociation constants, particularly on K_{d1} (data not shown). It is beyond the scope of the present paper to undertake extensive kinetics analysis of the ATPase reaction, and more data points (particularly at ATP concentration below K_{d1}) would be required to accurately fit the kinetic parameters of the reaction scheme. Nonetheless, Figure 2 shows that CFX and MccB17 have distinct effects on the kinetics of the gyrase ATPase reaction.

Rate of ATP Hydrolysis as a Function of MccB17 Concentration. Saturation curves in inhibitor concentration (dose–response curves) were used to compare the potency of MccB17 with that of CFX in the DNA-dependent ATPase reaction. The rate of the DNA-dependent ATPase reaction was measured as a function of MccB17 concentration to estimate the apparent dissociation constant, K_d . MccB17 inhibited the ATPase reaction of gyrase in the presence of linear pBR322 DNA (Figure 3); data were fitted to the

hyperbolic equation:

$$\frac{\nu}{\nu_0} = \frac{\alpha L + K_d}{L + K_d} \quad (2)$$

where ν is the rate of the reaction, ν_0 is the initial rate in the absence of inhibitor, α is the ratio of rate at infinite inhibitor concentration (ν_∞) over the rate at zero inhibitor concentration (ν_0), L is the ligand (MccB17 or CFX) concentration, and K_d is the apparent dissociation constant for L . MccB17 inhibited the DNA-dependent ATPase activity of gyrase by ~40% at saturation ($\alpha = 0.6$) with an apparent K_d of $11 \pm 2 \mu\text{M}$ (Figure 3). We found that a saturating concentration of CFX could inhibit the ATPase reaction by ~50% with an apparent K_d of $70 \pm 9 \text{ nM}$, ~150-fold less than the K_d for MccB17 (Figure 3). When increasing concentrations of MccB17 were tested on a mutant enzyme containing GyrB with a MccB17-resistant mutation [Trp⁷⁵¹ to Arg; (8)], little or no inhibition by the toxin was seen (data not shown), supporting the idea that the inhibition observed with the wild-type enzyme is significant.

ATPase Reactions with Competing Inhibitors. Since MccB17 and CFX showed distinct levels of inhibition, we tested both inhibitors in the same ATPase reaction. When MccB17 concentration was varied in the presence of 0.05 or 2 μM CFX (Figure 4A), no additive effect was observed with CFX at the higher concentration; at the lower concentration, additional inhibition was seen in the presence of MccB17. The reverse experiment was carried out in which [CFX] was varied in the presence of 5 or 30 μM MccB17 (Figure 4B). In both cases, the addition of CFX caused increased inhibition of the ATPase activity to reach the level expected at high CFX concentrations. These data show that in the presence of excess CFX (2 μM ; Figure 4A) the effect of this inhibitor dominates, while in the presence of limiting CFX (0.05 μM ; Figure 4A) inhibition at low [MccB17] reflects partial inhibition by CFX, while at high [MccB17] the effect reflects the characteristic MccB17 rate. In no case was the effect of MccB17 and CFX additive; i.e., the inhibition never exceeded that found in the presence of excess CFX. These results suggest either that these two inhibitors have overlapping binding sites, i.e., the binding of one precludes the binding of the other, or that they share a common allosteric mechanism of inhibition of the ATPase reaction.

For comparison, novobiocin was tested in the same reaction with MccB17 or CFX (Figure 4C,D). We tested increasing concentrations of MccB17 or CFX in the ATPase reaction with or without 0.05 or 1 μM novobiocin. At saturation (1 μM), novobiocin completely inhibited the reaction, regardless of the presence of CFX or MccB17. At limiting novobiocin concentration (0.05 μM), both CFX and MccB17 caused additional inhibition of the ATPase reaction. At saturating CFX or MccB17 concentration, novobiocin could still produce additional inhibition. This suggests that novobiocin can bind to the enzyme at the same time as CFX and MccB17 and its effect dominates that of the two other inhibitors.

DNA Dependence of the MccB17-Characteristic ATPase Rate. In earlier work we used the ATPase reaction to probe the formation of the enzyme–DNA complex as a function of DNA concentration (32, 34) and found that the dependence

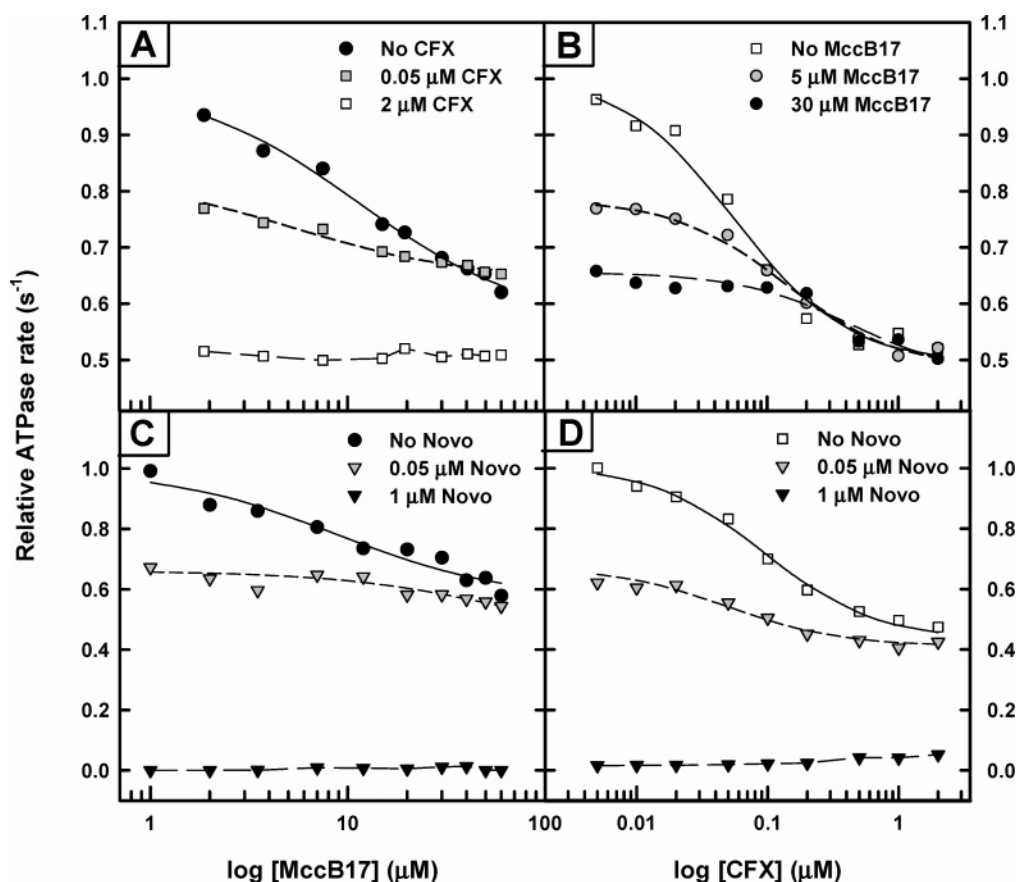


FIGURE 4: Competition between two inhibitors in the same ATPase assay. Various concentrations of MccB17 or CFX were tested on the ATPase reaction in the same conditions as in Figure 3. Where indicated, the reactions also included either CFX at 0.05 or 2 μ M, MccB17 at 5 or 30 μ M, or novobiocin at 0.05 or 1 μ M. ATPase activity is expressed relative to the rate in the absence of inhibitor (equal to 1 s⁻¹), and curves are from the fit to eq 2.

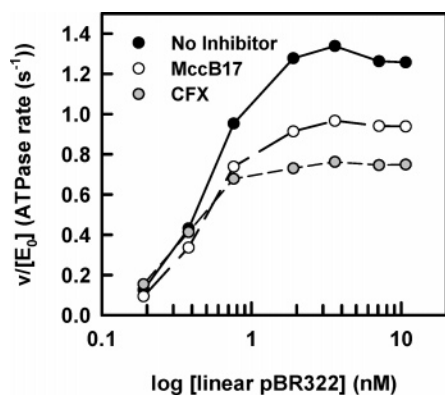


FIGURE 5: Dependence of the MccB17- or CFX-characteristic ATPase rate on linear DNA concentration. The reactions were incubated at 25 °C and contained 2 mM ATP, 48 nM gyrase, 0.5–30 μ g/mL linear pBR322, 5% Me₂SO, and, where indicated, 30 μ M MccB17 or CFX.

of the ATPase rate on DNA concentration is steeper in the presence of CFX than in its absence (34). In the present work, we wanted to see if the MccB17-characteristic rate was dependent on DNA concentration in the same way. Gyrase (48 nM) was incubated with various concentrations of linear pBR322 DNA, and ATPase rates were determined in the presence of 5% Me₂SO, with or without 30 μ M MccB17 or CFX (Figure 5). Data for the CFX-bound enzyme reached a plateau at a lower DNA concentration than those for the drug-free enzyme, with a CFX-characteristic rate corresponding to \sim 40% inhibition of the maximal rate without drug.

MccB17 displayed a characteristic rate distinct from that of CFX, corresponding to \sim 30% inhibition of the maximal rate obtained for the drug-free enzyme. Moreover, Figure 5 shows that, unlike CFX, the curve with MccB17 did not reach a plateau earlier than the one without inhibitor. These results indicate that, unlike CFX, MccB17 does not increase the binding affinity of gyrase for DNA. This finding is confirmed in the next section with short DNA fragments.

DNA Length Dependence of the MccB17-Characteristic ATPase Rate. Our previous work on the action of MccB17 on the DNA cleavage and supercoiling reactions of gyrase suggested an involvement of DNA strand passage for the toxin action (12). To find evidence for the requirement of strand passage in MccB17 action, we used the ATPase reaction of gyrase to probe the effect of DNA length on the inhibition by MccB17. We also tested CFX as a control, since the DNA length requirement for the effect of quinolone on the ATPase reaction is well-known (34). We performed the ATPase assays with linear DNA varying in concentration from 0.5 to 30 μ g/mL and in length ranging from 54 to 220 bp. These DNA fragments contain, approximately in the middle of the sequence (Figure 1), the preferred quinolone (27, 35, 36) and MccB17 (10) cleavage site of pBR322 at position 990 (Figure 6A,B) or, alternatively, the strong quinolone cleavage site from the Mu bacteriophage (Figure 6C,D) (36).

DNA fragments of less than 85 bp (54, 76 with the 990 site; Mu72 with the Mu site) were tested in the ATPase reaction, with or without MccB17 or CFX (Figure 6A,C).

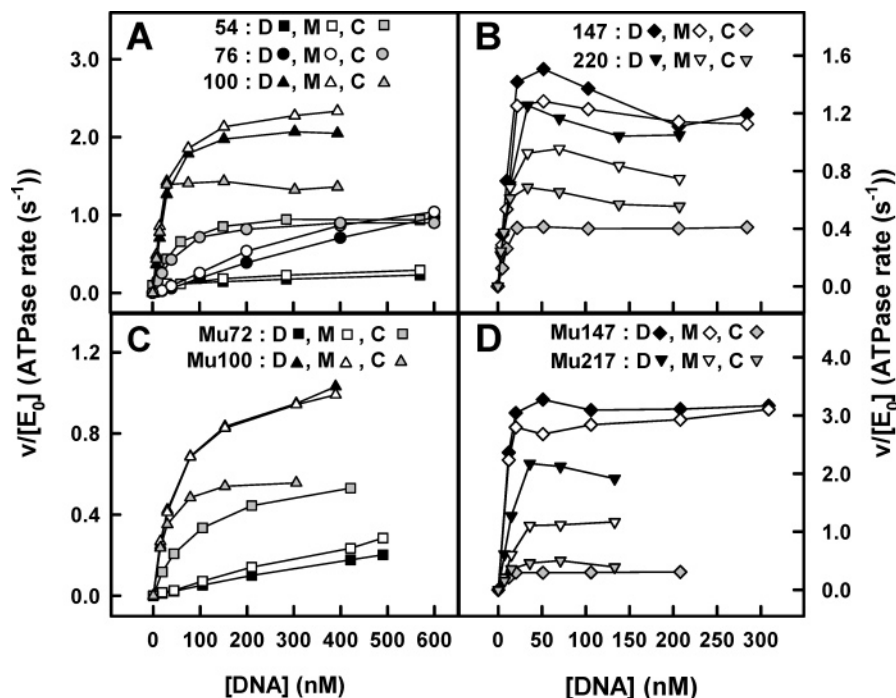


FIGURE 6: Dependence of the MccB17- or CFX-characteristic ATPase rate on length of linear DNA fragments. Conditions are the same as in Figure 5, except for the reactions with DNA fragments <100 bp where the gyrase concentration was increased to 80 nM. Linear DNA fragments contained, approximately in the middle of the sequence (Figure 1), the preferred quinolone cleavage site of pBR322 at position 990: (A) 54, 76, 100; (B) 147, 220; pMP1625 with the strong bacteriophage Mu site; (C) Mu72, Mu100; (D) Mu147, Mu217. D = Me₂SO only; M = 30 μ M MccB17; C = 30 μ M CFX.

At the highest DNA concentration tested in the assay (30 μ g/mL), very little stimulation of the ATPase reaction of the drug-free enzyme was observed with the 54 and the Mu72 DNA fragments, but a significant level of activation by the 76 bp DNA was reached, in good agreement with previous work where binding studies indicated a very weak interaction between gyrase and a 55 bp linear DNA fragment (32). In the presence of CFX, the ATPase rate was stimulated similarly with the 54 and 76 bp fragments, with a sharp increase at low DNA concentrations to reach a plateau at ~ 0.7 s⁻¹ with 200–280 nM (10 μ g/mL) DNA (Figure 6A). Similarly, CFX stimulated the ATPase rate with the Mu72 DNA, with a 4.4-fold enhancement at 210 nM (10 μ g/mL) DNA (Figure 6C). A similar stimulation of the ATPase activity of gyrase by CFX with DNA fragments as short as 20 bp was reported previously and can be explained by CFX stabilizing the interaction between gyrase and DNA (34). Unlike CFX, MccB17 was unable to significantly activate the ATPase reaction in the presence of the short DNA fragments of 54–76 bp (Figure 6A,C).

DNA fragments of 100 bp or more were able to fully activate the ATPase reaction, typically by ~ 15 -fold (data not shown), consistent with earlier work (32). Figure 6B shows that, with a 220 bp DNA from the 990 site, MccB17 and CFX inhibited the ATPase reaction to a level similar to the inhibition observed with full-length pBR322. With 70 nM (10 μ g/mL) Mu217 DNA (Mu site), MccB17 and CFX inhibited the ATPase reaction of gyrase respectively by $\sim 50\%$ and 80% (Figure 6D), hence a stronger inhibition compared to the one obtained with the long pBR322 DNA fragments containing the 990 site. The trends with a DNA length of 147 bp were remarkably different between MccB17 and CFX. At 100 nM (10 μ g/mL) 147 DNA (pBR322 site) or Mu147 DNA (Mu site), MccB17 inhibited the ATPase

reaction by only 10% and 8%, respectively, in sharp contrast with CFX, which strongly inhibited the reaction by 70% and 90%, respectively (Figure 6B,D). The most significant result was the total absence of inhibition by MccB17 when the DNA length was lowered to 100 bp, whereas the same reaction was still inhibited by CFX (Figure 6A,C). This result clearly shows that, despite activation of the gyrase ATPase reaction by a 100 bp DNA fragment, this length of DNA is not sufficient for the inhibition of the reaction by MccB17; i.e., the toxin needs a longer DNA fragment.

Various linear DNA lengths from 54 to 372 bp (with the preferred 990 or Mu cleavage sites at or near the center, Figure 1) were tested at a fixed concentration of 10 μ g/mL in the ATPase reaction of gyrase, and the effects of MccB17 and CFX were determined. Figure 7A shows that MccB17 requires a DNA length of more than ~ 150 bp to inhibit the ATPase reaction, in sharp contrast with CFX, which affected the ATPase reaction with all of the DNA fragments tested here. Moreover, this finding was not specific to a particular preferred nucleotide target sequence since the same DNA length requirement for MccB17 was found with DNA fragments surrounding both the 990 site of pBR322 and the strong gyrase cleavage site from bacteriophage Mu. The 198 bp DNA gave an anomalous result since MccB17 had no effect, even after increasing the DNA concentration up to 100 μ g/mL (data not shown). However, when we took a different nucleic acid sequence of the same size (198 bp) but outside the preferred gyrase 990 cleavage site, we found 34% inhibition of the ATPase by MccB17. We cannot easily explain the result found with the 198 bp DNA containing the 990 site from pBR322, but it is likely that the exact location(s) of gyrase on the DNA fragment can greatly influence the effect of MccB17 on the ATPase reaction. It is known that the DNA sequence specificity of gyrase is not

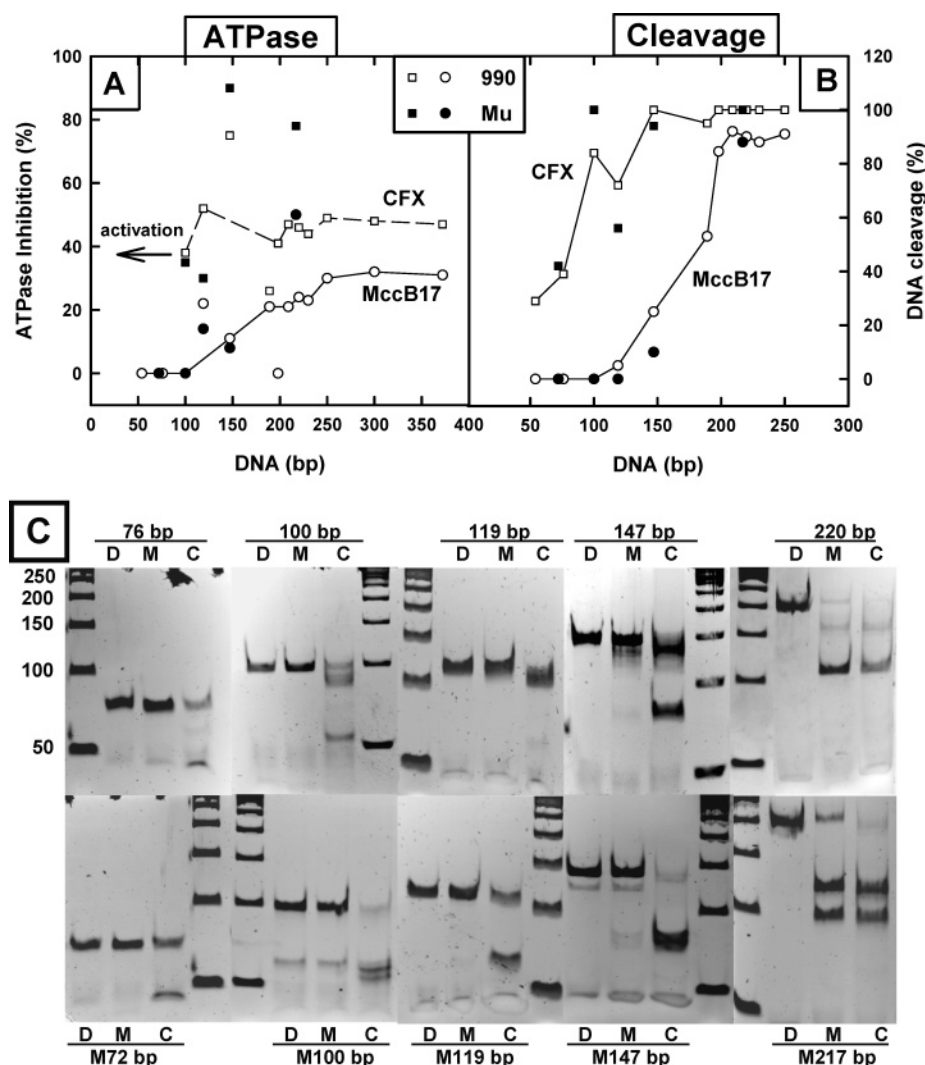


FIGURE 7: The action of MccB17 on the ATPase and DNA cleavage reactions of gyrase requires a DNA fragment longer than 150 bp. The reactions contained 40–80 nM (ATPase) or 200 nM (cleavage) gyrase, 2 mM ATP, 4–5% Me₂SO, and, where indicated, 30 μM MccB17 or CFX. Samples were incubated at 25 °C in the presence of 10 μg/mL linear DNA fragments, 54–372 bp, containing the preferred quinolone cleavage site from pBR322 at position 990 or from bacteriophage Mu (Figure 1). (A) The DNA length dependence of the MccB17- and CFX-induced inhibition (or activation) of the ATPase reaction. (B) The DNA length dependence of the MccB17- and CFX-induced DNA cleavage. (C) The pattern of DNA bands obtained from cleavage of the 72–220 bp fragments surrounding the 990 site of pBR322 (top gel) or the Mu site (bottom gel). D = Me₂SO only; M = 30 μM MccB17; C = 30 μM CFX.

very strict, and it is possible for the enzyme to bind at sites other than the well-known gyrase preferred sequence (37).

DNA Length Dependence of the MccB17-Induced DNA Cleavage. To complement the results found with the ATPase reaction, DNA cleavage assays were performed by incubating DNA gyrase with linear DNA fragments (containing the 990 or Mu preferred cleavage sites) from 54 to 250 bp, in the presence of 4% Me₂SO, with or without 30 μM MccB17 or CFX. The product of each reaction was run on an 8% polyacrylamide gel from which the percentage of DNA cleavage was quantified. Results for the cleavage reaction are presented in Figure 7B, next to the one for the ATPase reaction (Figure 7A) to facilitate comparison. The cleavage reaction shows approximately the same DNA length dependence for MccB17 action as the ATPase reaction, i.e., a requirement for a long DNA fragment of more than ~150 bp. In contrast, CFX could induce the cleavage of DNA as short as 54 bp, in good agreement with previous reports that showed quinolone-induced cleavage of a 20 bp DNA fragment (38, 39).

The pattern of DNA cleavage bands gives further information on the actual number of cleavage sites on the DNA and, hence, on the position of the enzyme on its DNA substrate. It has been suggested that cleavage site specificity with short DNA fragments is determined by the specific drug–DNA interactions, whereas with long DNA fragments the positioning of the DNA wrap around gyrase dictates the site of cleavage (39). Figure 7C illustrates the cleavage patterns of some of the DNA fragments used in this study. Overall, the major cleavage bands correspond to the preferred cleavage site observed previously with quinolones, at the 990 position of pBR322 (39) or at the strong gyrase site of bacteriophage Mu (28, 36, 40). However, particularly for the 990 site of pBR322, one or two secondary cleavage sites were found, as reported previously in the case of the enoxacin-induced DNA cleavage (36). The 189 and 198 bp DNAs were cleaved multiple times in the presence of both inhibitors; at least six to eight bands were visible on the gel (data not shown). Multiple cleavage of short DNA fragments in the presence of CFX has been reported previously (39). It is worth noting

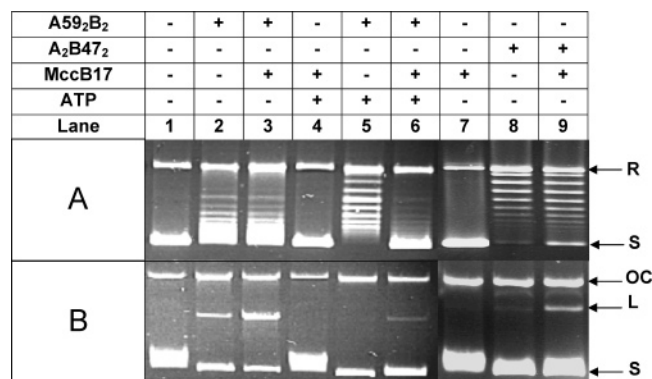


FIGURE 8: Effect of MccB17 on the reactions of DNA relaxation and DNA cleavage by A59₂B₂ and A₂B47₂ gyrases. The reactions contained 7.1 nM negatively supercoiled DNA, 2.5% or 3.3% Me₂SO, and, where indicated, 30 μM MccB17 and 1.7 mM ATP. Following incubation at 25 °C for 3–6 h, the samples were either not treated (top gel A) or treated (bottom gel B) with SDS and proteinase K, prior to analysis on agarose gels, without (A) or with (B) 1 μg/mL ethidium bromide. Lanes 1, 4, and 7 (from left): reaction without enzyme. Lanes 2 and 3: ATP-independent relaxation of DNA by 80 nM A59₂B₂. Lanes 5 and 6: ATP-dependent relaxation of DNA by 20 nM A59₂B₂. Lanes 8 and 9: ATP-independent relaxation of DNA by 47 nM A₂B47₂. DNA forms: R = relaxed; S = negatively supercoiled; OC = open circular; L = linear.

that when multiple secondary cleavage sites were present in the DNA (i.e., with 189 bp, 198 bp, linear pBR322 DNA; data not shown), the pattern of bands was very similar between MccB17 and CFX, suggesting that both inhibitors share the same cleavage site preference.

Effect of MccB17 on the Reactions of A59₂B₂ and A₂B47₂ Gyrases. The requirement for long (>150 bp) DNA fragments for the action of MccB17 on gyrase prompted us to investigate whether the DNA wrapping domain of GyrA is necessary for the MccB17 mechanism of action. Therefore, we tested the effect of MccB17 on the ATP-dependent and ATP-independent DNA relaxation activities of A59₂B₂ gyrase lacking the DNA wrapping domain of GyrA. In the control reaction with the full enzyme (A₂B₂; data not shown), MccB17 showed the slow inhibition of DNA supercoiling and the DNA cleavage complex stabilization observed previously (12). In the present conditions, MccB17 had little or no inhibitory effect on the ATP-independent relaxation of DNA by A59₂B₂ but induced a significant amount of DNA cleavage in this reaction (Figure 8, lanes 2 and 3). Note that the ATP-independent DNA relaxation by A59₂B₂ was a slow reaction and progressed little after 4 h incubation, even with an enzyme concentration 4 times higher than in the ATP-dependent DNA relaxation reaction. The poor inhibition by MccB17 of this ATP-independent DNA relaxation reaction may be due to insufficient enzyme turnover. MccB17 significantly inhibited the efficient ATP-dependent DNA relaxation by A59₂B₂ and, to a lesser extent than with the wild-type enzyme, induced DNA cleavage (Figure 8, lanes 5 and 6). These results indicate that MccB17 does not need the wrapping domain of GyrA for its mechanism of action on gyrase.

In another set of experiments, MccB17 was tested on the ATPase reaction of A59₂B₂ (data not shown). It has been shown previously that A59₂B₂ exhibits a preference for supercoiled DNA and has a reduced affinity for DNA compared to gyrase, but CFX stabilizes the relatively weak

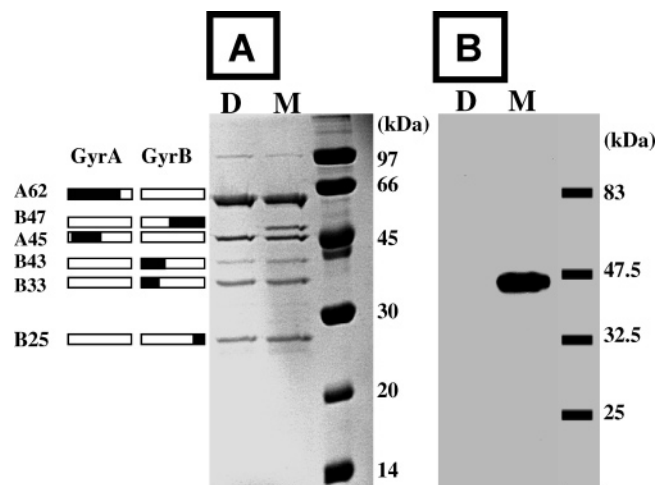


FIGURE 9: The MccB17-characteristic tryptic fingerprint. (A) Reactions containing 0.3 mg/mL A₂B₂, 0.24 mg/mL linear pBR322, 2.5 mM ATP, and 3.3% Me₂SO, with or without 40 μM MccB17, were incubated at 25 °C for 1 h. Samples were then treated with 100 μg/mL trypsin for 1 h at 37 °C and the products analyzed on SDS–PAGE. On the left is a diagrammatic representation of the gyrase fragment corresponding to each band (31, 41, 42). (B) Western blot of the gel from (A) with monoclonal antibody directed against GyrB47. D = Me₂SO only; M = 40 μM MccB17.

enzyme–DNA complex (19). We saw that linear pBR322 failed to stimulate the ATPase of A59₂B₂ due to the poor affinity of the enzyme for linear DNA, but the presence of CFX increased the ATPase activity by an order of magnitude (data not shown), in agreement with previous observations (19, 34). In contrast with CFX, MccB17 was unable to stimulate the low ATPase activity of A59₂B₂ (data not shown), presumably because MccB17 could not stabilize the weak interaction between the truncated enzyme and the linear form of DNA. Consistent with this, we could not see any cleavage of linear pBR322 in the presence of MccB17 and ATP when the A59₂B₂ enzyme replaced gyrase (data not shown). Note that, in contrast with linear DNA, MccB17 could induce cleavage in the DNA relaxation reaction by A59₂B₂ (Figure 8) because this enzyme interacts preferentially with the supercoiled form (19).

We also tested the effect of MccB17 on the DNA relaxation and DNA cleavage reactions of the A₂B47₂ gyrase lacking its ATPase domain. MccB17 could interact with the truncated gyrase as the toxin could significantly stabilize the formation of the cleavage complex and weakly inhibit the DNA relaxation reaction by A₂B47₂ (Figure 8, lanes 8 and 9). These results suggest that MccB17 does not require the ATPase domain of GyrB (GyrB43) for its action on gyrase.

Proteolytic Signature of MccB17. We have used limited trypsin proteolysis to probe the binding of MccB17 to DNA gyrase. The proteolytic pattern resulting from trypsin treatment of GyrA and GyrB in various experimental conditions is well documented (30, 31, 41, 42). Proteolysis of GyrA produces one major fragment of ~62 kDa corresponding to the N-terminal domain (41), and at high trypsin concentrations this fragment is broken down into a ~45-kDa fragment (31) that we observed in Figure 9. Proteolysis of GyrB produces three bands at 43, 33, and 25 kDa (41, 42) that we observed in Figure 9. When the enzyme–DNA complex was incubated with 40 μM MccB17 prior to trypsin treatment, one more fragment was produced, with an approximate size

of 47 kDa (Figure 9). Peptide mass fingerprint analysis from MALDI-TOF mass spectrometry identified 11 peptides covering ~40% of the C-terminal domain of GyrB, from residues 461 to 789; Western blot analysis also identified this fragment as the 47-kDa domain of GyrB (Figure 9). When gyrase was incubated with MccB17 in the absence of DNA or ATP, no protection of the 47-kDa domain was observed (data not shown), consistent with the findings of the ATPase reaction. In the presence of MccB17, this 47-kDa fragment was observed regardless of the type of DNA substrate used (linear, relaxed, or negatively supercoiled pBR322; data not shown) and with a trypsin concentration as high as 500 $\mu\text{g/mL}$, indicating its strong resistance to further degradation, as previously reported (41). We also tested the MccB17-resistant mutant of GyrB ($\text{Trp}^{751} \rightarrow \text{Arg}$) and found no extra 47-kDa fragment in the presence of MccB17 (data not shown).

DISCUSSION

In a previous paper (12), we showed that MccB17 had distinct effects on the DNA supercoiling and relaxation reactions and the DNA cleavage–religation equilibrium of gyrase, compared to the quinolone CFX. First, we found that MccB17 cannot block immediately the DNA supercoiling and relaxation reactions: inhibition by the toxin becomes visible when these reactions are run over an extended period of time. Second, kinetic simulations of the reactions of DNA cleavage and religation showed that MccB17 only enhances the cleavage of the second strand of DNA, i.e., the conversion of open circular DNA to linear DNA. Finally, we found that the effect of MccB17 on the DNA cleavage reaction of gyrase depends on the topology of the DNA substrate: when starting from relaxed DNA (supercoiling conditions), MccB17 can stabilize the cleavage complex only weakly in the absence of ATP but more efficiently with the nucleotide; the cleavage complex can be stabilized more efficiently in the absence of ATP if negatively supercoiled DNA (DNA relaxation conditions) replaces relaxed DNA. From these findings, we suggested that the mode of action of the toxin may involve inhibition of the DNA strand-passage process, possibly by interacting with the gyrase–DNA complex near the DNA gate.

The hypothesis of MccB17 inhibiting DNA strand passage by gyrase raises questions about the toxin's mode of action. Is DNA strand passage required? Are the DNA-wrapping domain and the ATPase domain of gyrase necessary? Where does it bind on gyrase? In this paper, our results show that MccB17 can inhibit the ATPase reaction of gyrase, provided that DNA and both subunits are present. Then, we probed the effect of DNA length on the action of MccB17 in the ATPase and DNA cleavage reactions of gyrase and showed that MccB17 requires a fragment of DNA of at least 150 bp [approximately the minimum length necessary for DNA to form a wrapped complex (43–45)]; this is evidence for the role of DNA strand passage in the mechanism of toxin action. We also found that the wrapping domain of GyrA and the ATPase domain of GyrB were not essential for MccB17 action, thus indicating that strand passage only is necessary for toxin action. Finally, MccB17 binding to the enzyme induces a protection of the C-terminal 47-kDa domain of GyrB, only when DNA and ATP were present.

Inhibition of the ATPase Reaction by MccB17. As with CFX (34), MccB17 could inhibit the ATPase reaction of gyrase only when DNA was present in the reaction. We found that the rate of ATP hydrolysis in the presence of MccB17 shows a near-hyperbolic dependence on [ATP] that is distinct from the toxin-free, the CFX-bound, and the CcdB-bound enzymes (refs 31 and 34 and Figure 2). Unlike novobiocin (29), but similar to CFX or CcdB (31), MccB17 partially inhibited the ATPase reaction: some activity remains at saturation with inhibitor. However, a noticeable difference is the absence of inhibition by MccB17 at [ATP] < 0.2 mM, in contrast with the three other inhibitors novobiocin, CFX, and CcdB (29, 31). The 2-fold decrease of K_M for ATP in the presence of MccB17 (i.e., MccB17 increased the affinity of gyrase for ATP), combined with the mild effect on V_{max} , may explain the apparent absence of inhibition by the toxin at low [ATP]. The apparent K_d for MccB17 ($\sim 10 \mu\text{M}$) in the ATPase reaction (Figure 3) is 1 order of magnitude higher than the IC_{50} of $1 \mu\text{M}$ found in the DNA cleavage reaction, whereas that for CFX ($\sim 70 \text{ nM}$) is lower than the IC_{50} of $0.2 \mu\text{M}$ reported earlier in the DNA cleavage reaction (10, 12). Similarly to the ATPase reaction, we found that the inhibition of the DNA supercoiling reaction also required a high concentration ($\sim 20 \mu\text{M}$) of MccB17 (data not shown). This distinction between MccB17 and CFX indicates a different mechanism of action at the molecular level. Competition experiments between MccB17 and CFX suggest that these inhibitors may have overlapping binding sites. However, MccB17 and CFX have very different structures, and it is unlikely that they have identical modes of binding to gyrase.

MccB17 Does Not Stabilize the Gyrase–DNA Interaction. In earlier work (32, 33), it was found that a minimum of $\sim 85 \text{ bp}$ DNA was required to fully activate the ATPase reaction; the effectiveness of long DNA fragments in stimulating the ATPase correlates with efficiency of their binding to the enzyme. A model was proposed in which at least two DNA-binding sites separated from each other on the enzyme must be occupied in order to stimulate the ATPase activity, consistent with the requirement for a G- and T-segment to be bound to the enzyme (46). In the present work, DNA fragments of various lengths were tested in the ATPase reaction, and our results are entirely consistent with these earlier experiments.

It has been shown that CFX can stabilize the weak interaction between gyrase and small DNA fragments, probably by increasing the enzyme affinity for the G-segment of DNA (38, 39). The present work provides evidence that MccB17 does not increase the affinity of gyrase for DNA, in sharp contrast with CFX. First, the dependence of the formation of the enzyme–DNA complex on [linear pBR322] was not steeper in the presence of MccB17 than in its absence (Figure 5). Second, when linear pBR322 was used as DNA substrate, MccB17 could not increase the weak ATPase activity of the A592B_2 enzyme (due to weak linear DNA binding), nor induce DNA cleavage in the reaction (data not shown). Finally, MccB17 was unable to stimulate the low gyrase ATPase activity in the presence of short DNA fragments of 54–76 bp (Figure 6).

The Action of MccB17 on Gyrase Requires a Linear DNA Longer than 150 bp. We found that MccB17 was unable to reach its maximal inhibitory effect on the ATPase reaction

of gyrase, unless DNA fragments of more than 150 bp were present in the reaction, in sharp contrast with CFX (Figure 7A). We believe that the difference between 85 and 150 bp (or more) reflects the difference in size of DNA required for ATPase stimulation and DNA strand passage, respectively. In other words, the critical requirement in DNA length by MccB17 strongly indicates that the toxin requires a DNA long enough, not only for activating the ATP hydrolysis but most importantly for allowing DNA strand passage through the enzyme.

It was found previously that in the presence of quinolones gyrase can cleave DNA fragments as short as 20 bp (38, 39), whereas CcdB-induced gyrase cleavage requires a DNA length of at least 165 bp (47). In good agreement with the ATPase reaction, our results on the DNA cleavage reaction demonstrated that, unlike CFX, but similarly to CcdB, MccB17-induced cleavage required a length of DNA of more than 150 bp (Figure 7B,C).

MccB17 Action Does Not Require the Wrapping and ATPase Domains of Gyrase. Among topoisomerases, gyrase is unique in its ability to negatively supercoil DNA, due to specific DNA wrapping by the C-terminal domain of GyrA. DNA cleavage experiments have been carried out with negatively supercoiled DNA and A64B₂ gyrase lacking its DNA-wrapping domain, and it was found that CcdB could not stabilize the cleavage complex (47). Unlike CcdB, we found that the DNA-wrapping domain of gyrase is not necessary for MccB17 action (Figure 8). Because of the significant effect of MccB17 on A59B₂, we tested the toxin on the ATP-dependent DNA relaxation and DNA decatenation reactions of topo IV (data not shown); we found no effect on decatenation and a weak inhibition on relaxation. Unlike CFX, MccB17 could not induce significant formation of a DNA–topo IV cleavage complex, suggesting that gyrase is the primary target of MccB17 in vivo. Note that Trp⁷⁵¹ of GyrB is not conserved but replaced by an Arg residue in topo IV, suggesting that the toxin may bind inefficiently to the enzyme.

We found that MccB17 could affect the A₂B47₂ enzyme reactions (Figure 8); thus, the ATPase domain (GyrB43) is not required and ATP hydrolysis is not mandatory for toxin action. This result indicates that the subtle effect of MccB17 observed above on the ATPase reaction is not through its direct binding at the ATPase domain of gyrase but is an allosteric effect from a binding site distant from the nucleotide-binding domain. From these experiments with the A59B₂ and A₂B47₂ enzymes, we can deduce that the MccB17 binding site is likely to involve one or both of the remaining domains of gyrase, i.e., GyrA59 and/or GyrB47.

The MccB17 Proteolytic Signature Corresponds to the C-Terminal 47-kDa Domain of GyrB47. Using limited trypsin proteolysis, we showed that MccB17 binding to the enzyme–DNA complex was associated with a characteristic proteolytic fingerprint involving a protection of the C-terminal 47-kDa domain of GyrB47. This proteolytic signature of MccB17 is reminiscent of that reported earlier for CFX, which also required DNA (41), but, unlike CFX, addition of ATP in the reaction was also mandatory. The CFX-induced fingerprint was shown to result from a drug-induced enzyme conformational change involving the GyrB subunit, not from a direct protection of the proteolytic site (41). Unlike CcdB (31), in the absence of nucleotide,

MccB17 did not increase the susceptibility of the GyrA 62-kDa fragment to proteolysis and did not induce the conversion of the 62-kDa fragment to a 49-kDa product. In the case of CcdB, this 49-kDa fragment was assumed to arise from the specific binding of CcdB at the Arg⁴²⁶ site in GyrA, and such an event seems unlikely with MccB17. In the presence of ATP, however, an additional fragment corresponding to the C-terminal 47-kDa domain of GyrB was also reported in the presence of CcdB (31), raising the possibility that the CcdB-, CFX-, and MccB17-stabilized cleavage complex may share a similar conformational change in gyrase.

Because the protection of the 47-kDa domain of gyrase was previously observed with CFX and CcdB, the fact that we saw the same pattern here with MccB17 does not prove that the toxin binds to this domain. However, it is striking that the mutant of gyrase resistant to MccB17 action, i.e., the Trp⁷⁵¹ → Arg, maps to the C-terminal 47-kDa domain, and the quinolone-resistant mutations associated with the GyrB subunit also map to this domain (48). Furthermore, there may be an additional relevance for MccB17 to target the GyrB47 fragment more specifically, as the toxin is highly bactericidal against a broad variety of phylogenetically related Gram-negative bacteria (2): the GyrB of *eubacteria* has a stretch of about 165 amino acids in the C-terminal half, which is lacking in other GyrB subunits and type II topoisomerases and which has been shown to play an important role in DNA binding and gyrase activity both in vivo and in vitro (49). Therefore, MccB17 may act on gyrase by binding at, or near, this stretch of important amino acids in GyrB47. However, attempts to directly measure binding of MccB17 to GyrB47 or to gyrase (A₂B₂) have been unsuccessful (data not shown). It is likely that a conformational change in GyrB47 only present during enzyme catalysis (i.e., DNA strand passage) is necessary for MccB17 binding. Consistent with this, we saw that the GyrB47 domain alone is highly susceptible to a low concentration of trypsin, and MccB17 could not protect it from proteolysis (data not shown). This is in sharp contrast with the high MccB17-induced resistance of GyrB47 to proteolysis when tested with the full enzyme subunits, DNA and ATP.

Model for the Interaction of MccB17 with DNA Gyrase. The present work has identified common features between MccB17 and CFX, like the requirement for DNA and both gyrase subunits for inhibition of ATPase activity and proteolytic signature and, possibly, overlapping binding sites on gyrase. But the mechanism of action of MccB17 resembles more that of CcdB (47, 50) in terms of requirement for ATP (12) and long DNA fragments. However, unlike CcdB (47), MccB17 does not need the wrapping domain of gyrase. Moreover, the formation of the MccB17-stabilized cleavage complex is reversible by treatment at 80 °C (data not shown), in contrast with the cleavage complex stabilized by CcdB (40, 50). Finally, our proteolysis experiments indicate that the two toxins do not bind in the same way to gyrase.

Several methods have established that the extent of interaction between gyrase and DNA involves a DNA segment of 130–140 bp (44–46). In addition, it was found that DNA gyrase can supercoil DNA circles as small as 174 bp (43). Therefore, we believe that the minimum DNA size requirement (at least 150 bp) found in the present work for

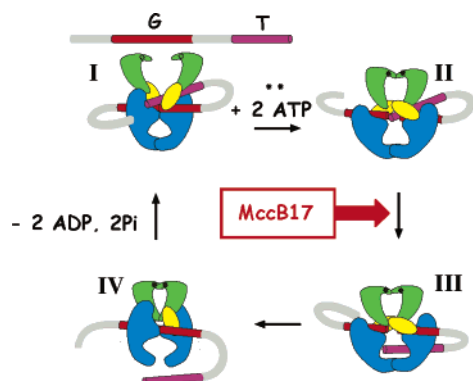


FIGURE 10: Model for the interaction of MccB17 with DNA gyrase during strand passage. A schematic representation of the gyrase supercoiling reaction is shown, with the "entry gate" at the top (GyrB43 ATP-operated clamp in green), the "DNA gate" in the middle, and the "exit gate" at the bottom (GyrB47 in yellow and GyrA59 in blue). The C-terminal domain of GyrA is not shown for clarity. The solid bar (gray) represents double-stranded DNA with the segment of DNA that is cleaved (G segment) in red and the segment of DNA that is transported through the enzyme (T segment) in purple. To perform strand passage, gyrase undergoes conformational changes from a closed state (I) to open states (II and III). From the present work, we can infer that the action of MccB17 on gyrase requires strand passage through the enzyme by targeting a conformation of gyrase resembling steps II or III. The DNA wrapping domain (omitted in the figure) is not required for MccB17 action. Although not shown, MccB17 can also interfere with the DNA relaxation reaction by gyrase which can be considered as the reverse process of the one depicted in the figure: in the absence of nucleotide, the T-segment can enter from the bottom gate and pass through the enzyme.

the action of MccB17 matches reasonably well the expected DNA size required for an extended gyrase–DNA interaction allowing T-segment passage and enzyme turnover. At present, we can only speculate on the mode of binding of MccB17 to gyrase, since only one mutant (the Trp⁷⁵¹ → Arg mutation in GyrB47) is known to confer resistance to MccB17 (8). In the case of the toxin CcdB, it is reasonable to think about a model in which the small protein would require an open gate conformation of gyrase to have access to its binding site, since it has been proposed that the CcdB dimer binds into the central hole of the 59-kDa N-terminal fragment of GyrA, after disruption of the head dimer interface of GyrA (51). As for CcdB, one can propose a model in which MccB17 needs strand passage to have access to its binding site within the central enzyme cavity. However, in the homologous domain of GyrB47 in the yeast topo II structure (B' domain), the residue corresponding to Trp⁷⁵¹ (Arg⁶¹⁴) is apparently not within the central cavity, regardless of whether it is the open, intermediate, or closed conformation of the enzyme (52, 53). We suggest that MccB17 traps a transient intermediate state of the gyrase reaction only present during DNA strand passage, as has been proposed for CcdB (40); such a mode of action is depicted in Figure 10. We can speculate that the hydrophobic nature of the MccB17 molecule suggests that it binds a hydrophobic surface of the protein that is only exposed during the strand passage cycle. Interestingly, rotation of the B' domains of yeast topo II has been proposed by comparing different enzyme structures (open, intermediate, and closed), and it was suggested that the reorganization of this domain may assist the transport of the T-segment as the enzyme approaches its open conformation (53). It is possible that,

similar to the topo II B' domain, the movement of GyrB47 during strand passage reveals a suitable surface for the binding of MccB17. Further experiments will be required to elucidate the molecular details of this model.

ACKNOWLEDGMENT

We thank Yi-der Chen for helpful discussions and the John Innes Centre Proteomics Facility for MALDI-TOF mass spectrometry analysis.

REFERENCES

- Asensio, C., Pérez-Díaz, J. C., Martínez, M. C., and Baquero, F. (1976) A new family of low molecular weight antibiotics from enterobacteria, *Biochem. Biophys. Res. Commun.* 69, 7–14.
- Destoumieux-Garzon, D., J., P., and Rebuffat, S. (2002) Focus on modified microcins: structural features and mechanisms of action, *Biochimie* 84, 511–519.
- Liu, J. (1994) Microcin B17: posttranslational modifications and their biological implications, *Proc. Natl. Acad. Sci. U.S.A.* 91, 4618–4620.
- Yorgey, P., Lee, J., Kordel, J., Vivas, E., Warner, P., Jebaratnam, D., and Kolter, R. (1994) Posttranslational modifications in microcin B17 define an additional class of DNA gyrase inhibitor, *Proc. Natl. Acad. Sci. U.S.A.* 91, 4519–4523.
- Bayer, A., Freund, S., and Jung, G. (1995) Post-translational heterocyclic backbone modifications in the 43-peptide antibiotic microcin B17. Structure elucidation and NMR study of a ¹³C, ¹⁵N-labelled gyrase inhibitor, *Eur. J. Biochem.* 234, 414–426.
- Li, Y. M., Milne, J. C., Madison, L. L., Kolter, R., and Walsh, C. T. (1996) From peptide precursors to oxazole and thiazole-containing peptide antibiotics: microcin B17 synthase, *Science* 274, 1188–1193.
- Sinha Roy, R., Gehring, A. M., Milne, J. C., Belshaw, P. J., and Walsh, C. T. (1999) Thiazole and oxazole peptides: biosynthesis and molecular machinery, *Nat. Prod. Rep.* 16, 249–263.
- Vizan, J. L., Hernandez-Chico, C., del Castillo, I., and Moreno, F. (1991) The peptide antibiotic microcin B17 induces double-strand cleavage of DNA mediated by *E. coli* DNA gyrase, *EMBO J.* 10, 467–476.
- Herrero, M., and Moreno, F. (1986) Microcin B17 blocks DNA replication and induces the SOS system in *Escherichia coli*, *J. Gen. Microbiol.* 132, 393–402.
- Heddle, J. G., Blance, S. J., Zamble, D. B., Hollfelder, F., Miller, D. A., Wentzell, L. M., Walsh, C. T., and Maxwell, A. (2001) The antibiotic microcin B17 is a DNA gyrase poison: characterisation of the mode of inhibition, *J. Mol. Biol.* 307, 1223–1234.
- Zamble, D. B., Miller, D. A., Heddle, J. G., Maxwell, A., Walsh, C. T., and Hollfelder, F. (2001) In vitro characterization of DNA gyrase inhibition by microcin B17 analogs with altered bis-heterocyclic sites, *Proc. Natl. Acad. Sci. U.S.A.* 98, 7712–7717.
- Pierrat, O. A., and Maxwell, A. (2003) The action of the bacterial toxin microcin B17. Insight into the cleavage-religation reaction of DNA gyrase, *J. Biol. Chem.* 278, 35016–35023.
- Champoux, J. J. (2001) DNA topoisomerases: structure, function, and mechanism, *Annu. Rev. Biochem.* 70, 369–413.
- Corbett, K. D., and Berger, J. M. (2004) Structure, molecular mechanisms, and evolutionary relationships in DNA topoisomerases, *Annu. Rev. Biophys. Biomol. Struct.* 33, 95–118.
- Roca, J., and Wang, J. C. (1992) The capture of a DNA double helix by an ATP-dependent protein clamp: a key step in DNA transport by type II DNA topoisomerases, *Cell* 71, 833–840.
- Morais Cabral, J. H., Jackson, A. P., Smith, C. V., Shikotra, N., Maxwell, A., and Liddington, R. C. (1997) Structure of the DNA breakage-reunion domain of DNA gyrase, *Nature* 388, 903–906.
- Corbett, K. D., Shultzaberger, R. K., and Berger, J. M. (2004) The C-terminal domain of DNA gyrase A adopts a DNA-bending β -pinwheel fold, *Proc. Natl. Acad. Sci. U.S.A.* 101, 7293–7298.
- Wigley, D. B., Davies, G. J., Dodson, E. J., Maxwell, A., and Dodson, G. (1991) Crystal structure of an N-terminal fragment of the DNA gyrase B protein, *Nature* 351, 624–629.
- Kampranis, S. C., and Maxwell, A. (1996) Conversion of DNA gyrase into a conventional type II topoisomerase, *Proc. Natl. Acad. Sci. U.S.A.* 93, 14416–14421.

20. Brown, P. O., Peebles, C. L., and Cozzarelli, N. R. (1979) A topoisomerase from *Escherichia coli* related to DNA gyrase, *Proc. Natl. Acad. Sci. U.S.A.* 76, 6110–6114.
21. Gellert, M., Fisher, L. M., and O'Dea, M. H. (1979) DNA gyrase: purification and catalytic properties of a fragment of gyrase B protein, *Proc. Natl. Acad. Sci. U.S.A.* 76, 6289–6293.
22. Maxwell, A. (1997) DNA gyrase as a drug target, *Trends Microbiol.* 5, 102–109.
23. Maxwell, A., and Howells, A. J. (1999) in *DNA Topoisomerase Protocols, Volume 1: DNA Topology and Enzymes*, pp 135–144, Humana Press, Totowa, NJ.
24. Reece, R. J., and Maxwell, A. (1991) The C-terminal domain of the *Escherichia coli* DNA gyrase A subunit is a DNA-binding protein, *Nucleic Acids Res.* 19, 1399–1405.
25. Smith, C. V. (1998) Investigating the mechanism and energy coupling of DNA gyrase, Ph.D. Thesis, Department of Biochemistry, University of Leicester, Leicester.
26. Sinha Roy, R., Kelleher, N. L., Milne, J. C., and Walsh, C. T. (1999) In vivo processing and antibiotic activity of microcin B17 analogs with varying ring content and altered bisheterocyclic sites, *Chem. Biol.* 6, 305–318.
27. Fisher, L. M., Mizuuchi, K., O'Dea, M. H., Ohmori, H., and Gellert, M. (1981) Site-specific interaction of DNA gyrase with DNA, *Proc. Natl. Acad. Sci. U.S.A.* 78, 4165–4169.
28. Pato, M. L., Howe, M. M., and Higgins, N. P. (1990) A DNA gyrase-binding site at the center of the bacteriophage Mu genome is required for efficient transposition, *Proc. Natl. Acad. Sci. U.S.A.* 87, 8716–8720.
29. Ali, J. A., Jackson, A. P., Howells, A. J., and Maxwell, A. (1993) The 43-kDa N-terminal fragment of the gyrase B protein hydrolyses ATP and binds coumarin drugs, *Biochemistry* 32, 2717–2724.
30. Reece, R. J., and Maxwell, A. (1989) Tryptic fragments of the *Escherichia coli* DNA gyrase A protein, *J. Biol. Chem.* 264, 19648–19653.
31. Kampranis, S. C., Howells, A. J., and Maxwell, A. (1999) The interaction of DNA gyrase with the bacterial toxin CcdB: evidence for the existence of two gyrase-CcdB complexes, *J. Mol. Biol.* 293, 733–744.
32. Maxwell, A., and Gellert, M. (1984) The DNA dependence of the ATPase activity of DNA gyrase, *J. Biol. Chem.* 259, 14472–14480.
33. Maxwell, A., Rau, D. C., and Gellert, M. (1986) in *Biomolecular stereodynamics III. Proceedings of the fourth conversation in the discipline of biomolecular stereodynamics* (Sarma, R. H., and Sarma, M. H., Eds.) pp 137–146, Adenine Press, Albany, NY.
34. Kampranis, S. C., and Maxwell, A. (1998) The DNA gyrase-quinolone complex—ATP hydrolysis and the mechanism of DNA cleavage, *J. Biol. Chem.* 273, 22615–22626.
35. Dobbs, S. T., Cullis, P. M., and Maxwell, A. (1992) The cleavage of DNA at phosphorothioate internucleotidic linkages by DNA gyrase, *Nucleic Acids Res.* 20, 3567–3573.
36. Oram, M., Howells, A. J., Maxwell, A., and Pato, M. L. (2003) A biochemical analysis of the interaction of DNA gyrase with the bacteriophage Mu, pSC101 and pBR322 strong gyrase sites: the role of the DNA sequence in modulating gyrase supercoiling and biological activity, *Mol. Microbiol.* 50, 333–347.
37. Lockshon, D., and Morris, D. R. (1985) Sites of reaction of *Escherichia coli* DNA gyrase on pBR322 *in vivo* as revealed by oxolinic acid-induced plasmid linearization, *J. Mol. Biol.* 131, 63–74.
38. Gmünder, H., Kuratli, K., and Keck, W. (1997) In the presence of subunit A inhibitors DNA gyrase cleaves DNA fragments as short as 20 bp at specific sites, *Nucleic Acids Res.* 25, 604–611.
39. Cove, M. E., Tingey, A. P., and Maxwell, A. (1997) DNA gyrase can cleave short DNA fragments in the presence of quinolone drugs, *Nucleic Acids Res.* 25, 2716–2722.
40. Scheirer, K., and Higgins, N. P. (1997) The DNA cleavage reaction of DNA gyrase. Comparison of stable ternary complexes formed with enoxacin and CcdB protein, *J. Biol. Chem.* 272, 27202–27209.
41. Kampranis, S. C., and Maxwell, A. (1998) Conformational changes in DNA gyrase revealed by limited proteolysis, *J. Biol. Chem.* 273, 22606–22614.
42. Kampranis, S. C., Gormley, N. A., Tranter, R., Orphanides, G., and Maxwell, A. (1999) Probing the binding of coumarins and cyclothialidines to DNA gyrase, *Biochemistry* 38, 1967–1976.
43. Bates, A. D., and Maxwell, A. (1989) DNA gyrase can supercoil DNA circles as small as 174 base pairs, *EMBO J.* 8, 1861–1866.
44. Orphanides, G., and Maxwell, A. (1994) Evidence for a conformational change in the DNA gyrase-DNA complex from hydroxyl radical footprinting, *Nucleic Acids Res.* 22, 1567–1575.
45. Liu, L. F., and Wang, J. C. (1978) DNA-DNA gyrase complex: the wrapping of the DNA duplex outside the enzyme, *Cell* 15, 979–984.
46. Heddle, J. G., Mittelheiser, S., Maxwell, A., and Thomson, N. H. (2004) Nucleotide binding to DNA gyrase causes loss of the DNA wrap, *J. Mol. Biol.* 337, 597–610.
47. Critchlow, S. E., O'Dea, M. H., Howells, A. J., Couturier, M., Gellert, M., and Maxwell, A. (1997) The interaction of the F plasmid killer protein, CcdB, with DNA gyrase: Induction of DNA cleavage and blocking of transcription, *J. Mol. Biol.* 273, 826–839.
48. Yamagishi, J., Yoshida, H., Yamyoshi, M., and Nakamura, S. (1986) Nalidixic acid-resistant mutations of the *gyrB* gene of *Escherichia coli*, *Mol. Gen. Genet.* 204, 367–373.
49. Chatterji, M., Unniraman, S., Maxwell, A., and Nagaraja, V. (2000) The additional 165 amino acids in the B protein of *Escherichia coli* DNA gyrase have an important role in DNA binding, *J. Biol. Chem.* 275, 22888–22894.
50. Bernard, P., Kézdy, K. E., Van Melderen, L., Steyaert, J., Wyns, L., Pato, M. L., Higgins, N. P., and Couturier, M. (1993) The F plasmid CcdB protein induces efficient ATP-dependent DNA cleavage by gyrase, *J. Mol. Biol.* 234, 534–541.
51. Loris, R., Dao-Thi, M.-H., Bahassi, E. M., Van Melderen, L. V., Poortmans, F., Liddington, R. C., Couturier, M., and Wyns, L. (1999) Crystal structure of CcdB, a topoisomerase poison from *E. coli*, *J. Mol. Biol.* 285, 1667–1677.
52. Berger, J. M., Gamblin, S. J., Harrison, S. C., and Wang, J. C. (1996) Structure and mechanism of DNA topoisomerase II, *Nature* 379, 225–232.
53. Fass, D., Bogden, C. E., and Berger, J. M. (1999) Quaternary changes in topoisomerase II may direct orthogonal movements of two DNA strands, *Nat. Struct. Biol.* 6, 322–326.
54. Morgan, G. J., Hatfull, G. F., Casjens, S., and Hendrix, R. W. (2002) Bacteriophage Mu genome sequence: analysis and comparison with Mu-like prophages in *Haemophilus*, *Neisseria* and *Deinococcus*, *J. Mol. Biol.* 317, 337–359.

BI0478751